Deep Resources Engineering 1 (2024) 100005

Contents lists available at ScienceDirect

Deep Resources Engineering

journal homepage: www.keaipublishing.com/en/journals/deepre/

An improved method to calculate the rock brittleness index PEECR based on linear energy storage law

Fengqiang Gong [a,b,c,*], Yiru Zuo [a,b], Song Luo [c], Yunliang Wang [c,d]

[a] School of Civil Engineering, Southeast University, Nanjing 211189, China
[b] Southeast University-Monash University joint graduate school, Southeast University, Suzhou, Jiangsu 215123, China
[c] School of Resources and Safety Engineering, Central South University, Changsha 410083, China
[d] EOST-ITES, Universite de Strasbourg, Strasbourg 67000, France

ARTICLE INFO

Keywords:
Rock brittleness index
Linear energy storage law
Peak elastic strain energy
Triaxial cyclic loading-unloading compression test

ABSTRACT

The peak elastic strain energy consumption ratio (PEECR) is a rock brittleness index proposed by Gong and Wang. In the present study, based on the linear energy storage law of rock under triaxial compression, a new method was proposed to calculate the PEECR. The PEECR uses a simplified method to calculate the peak elastic strain energy. To solve this problem accurately, triaxial cyclic loading-unloading compression tests were carried out on shale. Strain energy parameters were calculated from the test curves. The results show that there is a linear relationship between the elastic strain energy and input strain energy, indicating that the linear energy storage law in rock is applicable to triaxial compression state. The universality of the linear energy storage law of rock under triaxial compression is also verified by the data in the published literature. Then, the peak elastic strain energy can be accurately determined using the linear energy storage law, and the PEECR is improved based on this. Finally, the PEECR and the improved PEECR were compared using the triaxial cyclic loading-unloading compression tests on three rocks (shale, red sandstone and granite), and the improved PEECR was compared with 11 existing energy-based brittleness indexes. The results show that the improved PEECR can further reflect the rock brittleness more accurately.

1. Introduction

Rock brittleness is necessary to judge in projects such as oil exploration and tunnel construction. Therefore, many researchers in related fields have proposed many judgment criteria for rock brittleness, i.e., the brittleness index. These brittleness indexes are defined based on strength [1,9], rock fracture angle [9], mechanical parameters [9,11], stress-strain curve [3,13,14,27,28,32], and mineral composition [10], etc. [22,23] reviewed in detail the research progress of rock brittleness indices and their applications to different fields of rock engineering. It is known that the failure process of rock is always accompanied by the energy storage, dissipation, and conversion [30]. Therefore, increasing researchers have studied the energy evolution characteristics during rock failure to evaluate rock brittleness, and established various brittleness indexes from different perspectives [12,2,24–26,29,7]. The 11 existing rock brittleness indexes based on energy are summarized in Table 1, including their definitions and characteristics. It can be seen from Table 1 that BI_1-BI_{11} have some limitations, which affects the accuracy of rock brittleness evaluation. BI_1 does not take into account the post-peak energy, which also has a large impact on the brittleness of the rock. BI_2 and BI_3 simplify the relationship between the pre-peak elastic modulus and the post-peak deformation modulus, which affects the accuracy of judging the brittleness of rocks in individual cases. The formulas BI_4 and BI_5 are inappropriate and contradictory, and in some cases the judgment of the brittleness of the rock is not accurate. Although BI_6 takes into account the pre- and post-peak energy, it still includes the peak elastic strain energy in the calculation of fracture energy. When BI_7 and BI_8 judge the brittleness of shale under triaxial compression, the indexes change trend will be different with the increase of confining pressure, indicating that the judgment is occasionally inaccurate. BI_9 and BI_{10} use different multiplication factors, but some of them lack a theoretical basis. BI_{11} indicates that in the absolute brittle rock, the input strain energy is completely converted to elastic strain

Abbreviations: PEECR, The peak elastic strain energy consumption ratio.

Peer review under responsibility of Editorial Board of Deep Resources Engineering.

* Corresponding author at: School of Civil Engineering, Southeast University, Nanjing 211189, China.
E-mail address: fengqiangg@126.com (F. Gong).

https://doi.org/10.1016/j.deepre.2024.100005
Received 30 December 2023; Received in revised form 24 February 2024; Accepted 24 February 2024
Available online 11 March 2024

List of Symbols

U^{a}	Additional input strain energy
U^{f}	Total failure strain energy
U_{c}^{e}	Consumed elastic strain energy
U_{p}^{e}	Peak elastic strain energy
U_{p}^{d}	Peak Dissipated strain energy
U_{p}^{o}	Peak input strain energy
U_{r}^{e}	residual kinetic energy
σ_{p}	Peak strength
σ_{r}	Residual strength
U^{ei}	Peak elastic strain energy of the absolute brittle rock
BI_{ER}	A brittleness index based on the peak elastic strain energy consumption ratio (PEECR)
$BI_{I\text{-}ER}$	The improved BI_{ER} according to linear energy storage law
ε_{p}	Axial strain at the peak strength
ε_{r}	Axial strain at the beginning of the residual strength stage
ε_{u}	Axial strain when residual unloading stress is 0
$k\sigma_{p}$	Preset unloading stress
U_{k}^{oa}	Axial input energy at axial stress level is k
U_{k}^{ea}	Axial elastic strain energy at axial stress level is k
U_{k}^{da}	Axial dissipative strain energy at axial stress level is k
ε_{k}	Corresponding axial strain at axial stress level is k
ε_{d}^{k}	Axial plastic strain
k	The ratio of the current axial stress to the peak strength
σ_{k}	The axial stress corresponding to axial stress level k
U_{k}^{e}	Elastic strain energy
U_{k}^{d}	Dissipative strain energy
U_{k}^{o}	Input strain energy
a	Axial compression energy storage coefficient in the triaxial compression test
b	Fitting constant
c	Axial compression energy dissipation coefficient in the triaxial compression test
E	Elastic modulus

energy. However, the method of calculating the elastic strain energy of ideal brittle rock has not been verified and is not convincing. According to the previous studies on energy conversion of compressed rock, a new brittleness index named the peak elastic energy consumption ratio (PEECR) was proposed by [7], which can evaluate rock brittleness more accurately. In this existing study, the unloading curve is simplified into a straight line when calculating the peak elastic strain energy. As mentioned above in the energy-based brittleness index, all calculations of peak elastic strain energy are simplified methods. However, this calculation method is not accurate because the actual unloading curve is not straight. Therefore, it is necessary to propose an improved method to calculate the peak elastic strain energy.

In this study, the relationships among input strain energy, elastic strain energy and dissipative strain energy of rock are deeply analyzed through the triaxial cyclic loading and unloading compression test, and the linear energy storage law is found. After verifying the universality of the linear energy storage law, the PEECR is improved based on the linear energy storage law, and the accuracy and scientificity of the improved brittleness index are compared and analyzed.

2. PEECR and the difference between the simplified unloading curve and actual unloading curve

PEECR comprehensively considers the effects of pre-peak elastic strain energy, failure strain energy and residual kinetic energy on rock brittleness. A schematic diagram of the calculation of the various energy parameters of PEECR is shown in Fig. 1. Hereinafter, PEECR is abbreviated as BI_{ER}.

When $\varepsilon_{u}>\varepsilon_{p}$, BI_{ER} is expressed as [7]

$$BI_{ER}=\frac{U_{p}^{e}-U^{f}-U_{r}^{e}}{U_{p}^{e}}=\frac{\sigma_{p}^{2}\Big/2E-\int_{\varepsilon_{r}}^{\varepsilon_{p}}\sigma d\varepsilon}{\sigma_{p}^{2}\Big/2E} \tag{1}$$

When $\varepsilon_{u}<\varepsilon_{p}$, we have [7]

$$BI_{ER}=\frac{U_{p}^{e}-U^{f}-U_{r}^{e}}{U_{p}^{e}}=\frac{\sigma_{p}^{2}\Big/2E-\int_{\varepsilon_{r}}^{\varepsilon_{p}}\sigma d\varepsilon-1\Big/2(\varepsilon_{p}-\varepsilon_{u})^{2}\times E}{\sigma_{p}^{2}\Big/2E} \tag{2}$$

where U_{p}^{e} is the peak elastic strain energy, U^{f} is the failure strain energy, U_{r}^{e} is the residual kinetic energy, σ_{p} is the peak strength of rock, E is the elastic modulus of rock, ε_{p} is the axial strain at peak strength, ε_{r} is the axial strain at the beginning of the residual strength stage, and ε_{u} is the axial strain at which the residual stress unloading is 0.

The larger the BI_{ER}, the greater the rock brittleness. The case where BI_{ER} reaches the maximum of 1 indicates that the rock will be destroyed immediately after reaching the peak point. The smaller the BI_{ER}, the greater the rock plasticity. Especially, when BI_{ER} is less than 0, the pre-peak elastic strain energy is insufficient to damage the rock and its plastic deformation is maintained, which requires more input energy. This indicates that the rock with a negative BI_{ER} has greater plasticity than ordinary rocks [7].

In the test, it is often impossible to unload the rock in time when it is loaded to the peak point. As a result, the unloading curve cannot be used to calculate the peak elastic strain energy [4]. At present, the commonly used method of calculating the peak elastic strain energy is to simplify the unloading curve to a straight line with a slope of the elastic modulus [12]. From Fig. 2, we can see a large gap between the actual unloading curve and the simplified unloading curve, which means there is an obvious difference between the simplify calculated elastic strain energy and actual elastic strain energy. Therefore, the accuracy of the traditional method needs to be verified. It is necessary to find a new method to accurately calculate the peak elastic strain energy. Based on the new method, BI_{ER} can be modified to improve the accuracy of rock brittleness evaluation.

3. Triaxial compression test of shale and calculation method of energy parameters

In order to obtain the energy storage and consumption law of rock under triaxial conditions, a series of triaxial cyclic loading and unloading compression tests were carried out on shale. The calculation methods of each energy parameter are also indicated.

3.1. Triaxial cyclic loading and unloading compression test

The triaxial cyclic loading and unloading compression test was conducted on the shale from Changning, Sichuan, China. A raw rock was processed into standard samples (φ50mm × 100mm), as shown in Fig. 3. The basic parameters of the shale samples meet the test requirements (Table 2). The test was carried out using the MTS 815 rock triaxial test system (Fig. 4). The maximum axial loading force of the testing machine can reach 2600 kN, the maximum confining pressure can reach 140 MPa, and the maximum osmotic pressure is 140 MPa. The axial and circumferential deformations of the rock samples were measured by axial and circumferential extensometers, respectively.

Table 1
Eleven existing rock brittleness indexes based on energy [7].

Rock brittleness indexes	Energy parameters	Characteristics
$BI_1 = \frac{U_p^e}{U_p^e + U_p^d}$ Hucka, Das [9]	U^a,U^f and U_c^e are the additional input energy, total failure energy and consumed elastic strain energy during the failure process, respectively. U_p^e,$U_p^d$and$U_r^e$are the peak elastic strain energy, peak dissipated energy and residual elastic strain energy, respectively. $\sigma_p$and$\sigma_r$are the peak strength and residual strength, respectively. $U^{ei}$is the peak elastic strain energy of the absolute brittle rock.	BI_1means that the more elastic strain energy is stored in rock during pre-peak stage, the more brittle the rock is. However, the post-peak energy evolution characteristic is not considered in this index, which also has a great impact on rock brittleness.
$BI_2 = \frac{U^f}{U_c^e}$ Tarasovn, Randolph [25]		BI_2implies post-peak energy evolution characteristics, the failure relies more on the elastic strain energy and less on additional input energy, the more brittle the rock is.BI_3means the less additional input energy is needed and the more stored elastic strain energy is consumed during the failure process, the more brittle the rock is. However,$BI_2$and$BI_3$are simplified as the relationship of the prepeak elastic modulus and postpeak deformation modulus in original article, which will definitely affect the judgment accuracy.
$BI_3 = \frac{U^a}{U_c^e}$ Tarasovn, Randolph [25]		
$BI_4 = \frac{U^f + U_p^d}{U_c^e + U_p^d}$ Ai et al., [2]		BI_4involves the impact of the prepeak dissipated energy on the brittleness comparing withBI_2. It is believed that the less dissipated energy is generated during the prepeak, the more brittle the rock is. BI_5signifies dissipated energy has a negative influence on the rock brittle failure. However, the formulas of$BI_4$and$BI_5$are unsuitable and paradoxical.
$BI_5 = \frac{U^a}{U_c^e + U_p^d}$ Ai et al., [2]		
$BI_6 = \frac{1}{2}\left(\frac{U_c^e}{U^f} + \frac{U_c^e}{U_p^e + U_p^d}\right)$ Kivi et al., [12]		$BI_6$was proposed considering both the prepeak and postpeak energy evolution characteristics. It is believed that more elastic strain energy is stored in the prepeak stage and used for failure in the postpeak stage, the rock is more brittle. Despite this index is considered comprehensively, there is still a problem: the fracture energy should be the area under the postpeak curve subtracting the residual elastic strain energy, but the fracture energy in this index also includes the peak elastic strain energy.
$BI_7 = \frac{U^a}{U_c^e} + \frac{U_p^e + U_p^d}{U_p^e}$ Song et al., [24]		BI_7means that the more stored elastic strain energy is consumed and less additional input energy is needed during the failure process, the more brittle the rock is.
$BI_8 = \frac{U_p^e}{U_p^e + U_p^d} \times \frac{U_c^e}{U^f} \times \left(1 - \frac{U_r^e}{U_p^e}\right)$ Li et al., [15]		BI_8considers the impact of residual elastic strain energy on brittleness. It is believed that the bigger proportion of the stored elastic strain energy is consumed for failure and the smaller is left, the more brittle the rock is.
$BI_9 = \frac{U_p^e}{U_p^e + U_p^d} \times \frac{U_c^e}{U^f}$ Li et al., [15]		$BI_9$is extremely similar toBI_6, they have the same physical meanings. But$BI_9$is expressed in the form of multiplication.
$BI_{10} = \frac{U_p^e}{U_p^e + U_p^d} \times \left(1 - \frac{U_p^d}{U_p^d + U^f}\right) \frac{\sigma_p - \sigma_r}{\sigma_p}$ Li et al., [16]		BI_{10}involves the dissipation rate of the failure energy. It is believed that the faster the failure energy is dissipated, the more brittle the rock is. However,BI_7,BI_8,BI_9andBI_{10}all join different factors with multiplication which lacks a theoretical basis.
$BI_{11} = \frac{U_p^e}{U^{ei}} \times \frac{U^f}{U^a}$ Li et al., [17]		BI_{11}means the input energy will totally transfer into elastic strain energy for the absolute brittle rock, and the more elastic strain energy is stored in the rock, the more brittle the rock is. However, the calculation method of the elastic strain energy for ideal brittle rocks was not verified and thus not convincing.
$BI_{12} = \frac{U_p^e - U^f - U_r^e}{U_p^e}$ Gong, Wang [7]		$BI_{12}$was defined as the dissipated proportion of peak elastic strain energy relative to failure energy and residual elastic strain energy (the maximum value of it is 1.0, which indicates the corresponding rock will fail immediately after reaching the peak strength)

Four confining pressures of 5 MPa, 10 MPa, 20 MPa, and 30 MPa were set in the test. The conventional triaxial compression test was firstly performed on the shale samples to measure the triaxial compressive strength σ_p and the residual strength σ_r under each confining pressure. In the test, the axial and circumferential stress were applied simultaneously at a loading rate of 0.05 MPa/s. When the circumferential stress reached the value of preset confining pressure, the circumferential stress was stopped and maintained at the current stress state. The axial stress proceeded at a loading rate of 0.05 kN/s until reaching the preset unloading stress $k\sigma_p$(k=0.1, 0.3, 0.5, 0.7, 0.85, 0.95). Then the axial stress began to unload at the same rate, when the axial stress was released to the value of confining pressure, the circumferential stress and the axial stress were unloaded simultaneously, until both reached 1 MPa (In order to prevent the rock specimen from failing at a pressure of 0, the stress is not unloaded to 0). The second cycle was then started with the same procedures as the first cycle. After the last loading and unloading cycle, the axial and circumferential stresses were loaded together again. When the hoop stress reached the value of preset confining pressure, the loading was stopped and the stress state was maintained. The axial stress continued, and passed the peak strength point, and reached the residual strength stage. When the axial stress was maintained at the residual strength and did not change, it was unloaded. When the axial stress reached the value of confining pressure, the circumferential stress is also unloaded until both stresses are unloaded to 0, and the test ends. The loading path for this test is shown in Fig. 5.

The stress-strain curves are shown in Fig. 6. It can be observed that the peak strength and residual strength gradually increase with the increasing confining pressure. In addition, the unloading curve does not coincide with the loading curve, with a certain space between them. When the stress of the unloading curve is 0, the corresponding strain is not 0. This shows that a part of energy is dissipated due to damage or plastic deformation during loading process, and the rock has a certain plastic deformation. With the increasing number of cycles, the plastic strain of the rock gradually increases. It shows that the irreversible plastic deformation of rock increases gradually with the loading. In addition, during each cycle of loading and unloading under each confining pressure, the secondary loading curve just passed the last unloading point, and then still increased along the trend of the original

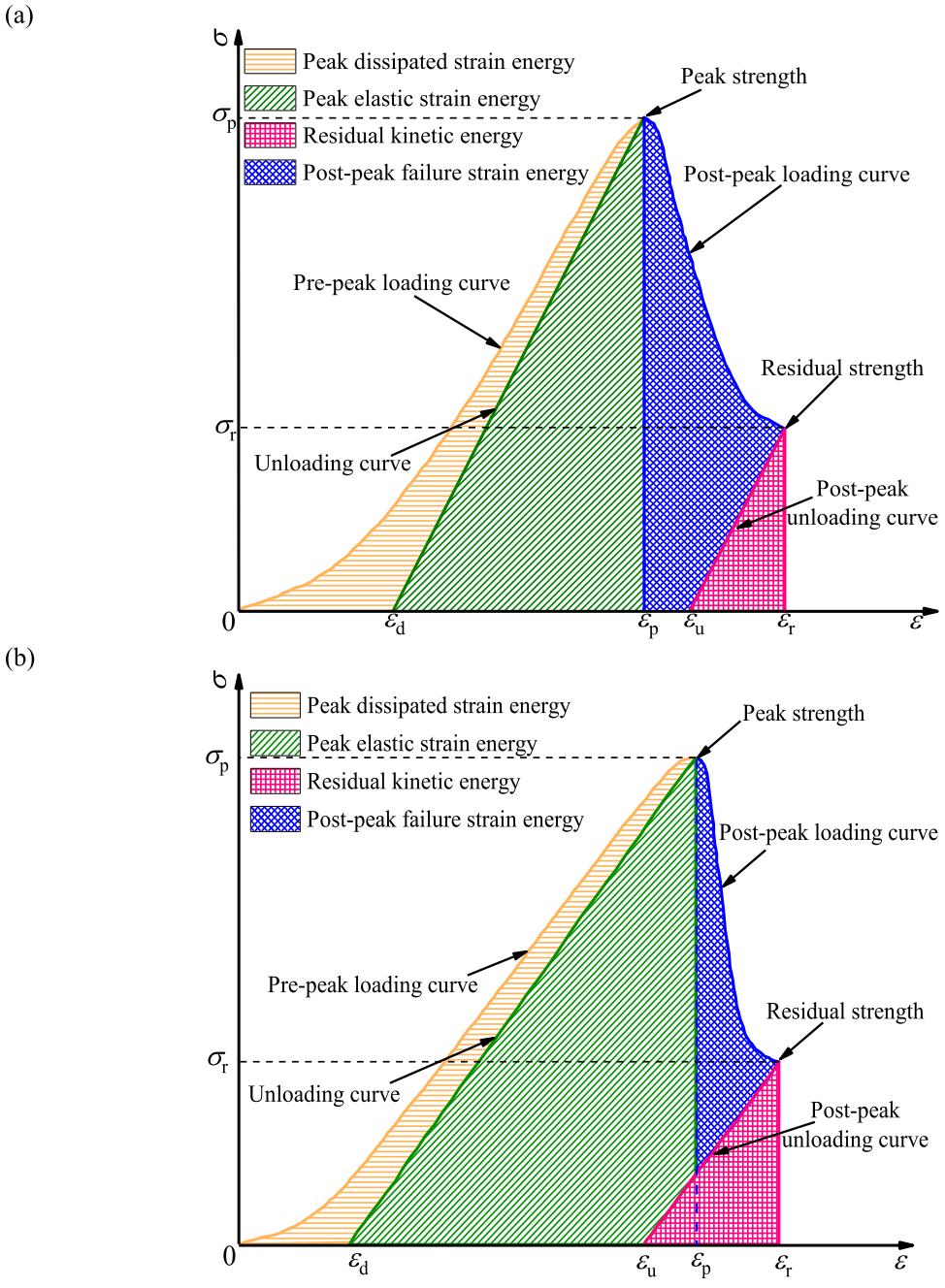

Fig. 1. Schematic diagram of energy distribution during rock deformation and failure: **(a)** $\varepsilon_u > \varepsilon_p$, and **(b)** $\varepsilon_u < \varepsilon_p$ [25].

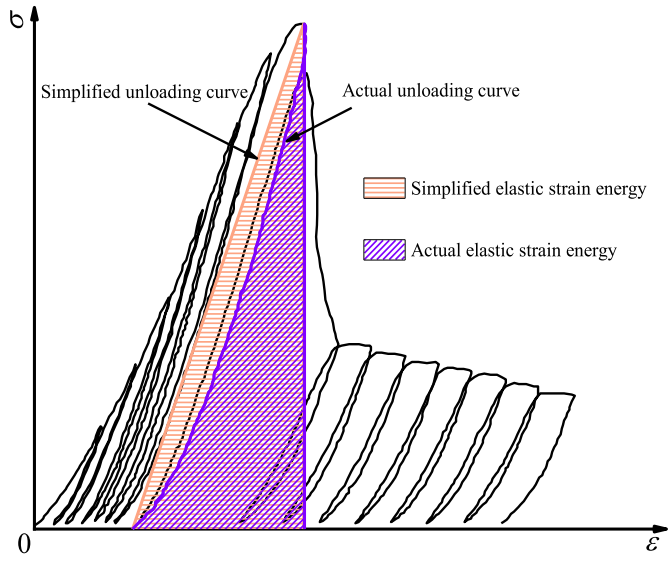

Fig. 2. Comparison of simplified unloading curve and actual unloading curve at peak value in triaxial cyclic loading and unloading compression test of rock.

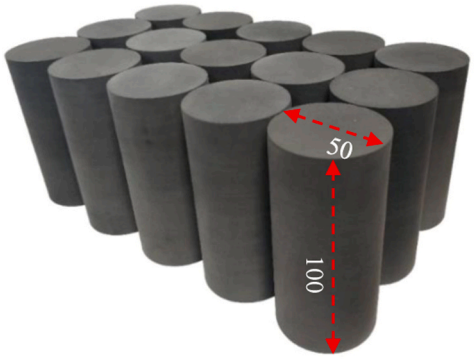

Fig. 3. The processed shale specimens [7].

Table 2
The basic parameters of shale specimens.

Density/ (g·cm^{-3})	P-wave velocity/ (m·s^{-1})	Elastic modulus/(GPa)	Uniaxial compressive strength/(MPa)
2.49	4074.27	19.17	167.65

loading curve. This shows that the cyclic loading and unloading process has little effect on the stress-strain curves of the rock.

3.2. Calculation method of strain energy parameters

Under triaxial compression conditions, many scholars have neglected the study of energy storage and dissipation characteristics of rock [8, 23]. In fact, according to energy storage and dissipation, a more accurate method for calculating the peak elastic strain energy and dissipative strain energy can be proposed, which can also improve the scientificity and accuracy of the BI_{ER}. The influence of radial load is not considered in this study, and the influence of radial load on the calculation still needs to be further studied. Therefore, only the calculation method of axial strain energy is proposed below.

The strain energy parameters are calculated by

$$U_k^{oa} = \int_0^{\varepsilon_k} \sigma d\varepsilon \tag{3}$$

$$U_k^{ea} = \int_{\varepsilon_d^k}^{\varepsilon_k} \sigma d\varepsilon \tag{4}$$

$$U_k^{da} = \int_0^{\varepsilon_k} \sigma d\varepsilon - \int_{\varepsilon_d^k}^{\varepsilon_k} \sigma d\varepsilon \tag{5}$$

where U_k^{oa}, U_k^{ea},U_k^{da}, and ε_k are the axial input energy, the axial elastic strain energy, the axial dissipative strain energy, and the axial strain at the axial stress level k respectively; ε_d^k is the axial plastic strain, the axial stress level k is the ratio of the current axial stress to the peak strength, and the axial stress corresponding to the axial stress level k is σ_k

4. Linear energy storage and dissipation law under the condition of rock triaxial cyclic loading and unloading compression

According to the experimental data obtained from the triaxial cyclic loading and unloading compression test above, it can be found that there is a certain law in the dissipation of rock energy. In this study, the data curve was fitted, the linear energy storage law was obtained, and its universality was verified. Subsequently, an improvement was proposed for the calculation method of energy parameters.

4.1. Linear energy storage and dissipation laws of rock under triaxial compression

To deeply study the energy storage and dissipation characteristics of rock, the relationship between the input strain energy, elastic strain energy and dissipative strain energy was analyzed according to the results of the triaxial cyclic loading and unloading tests (Fig. 6). Further, the data in the figure were fitted, and the fitted curve is shown in the Fig. 7 (in order to improve the reliability of the fitting results, (0, 0) points were added during fitting).

As shown in Fig. 7, it can be observed that a linear relationship occurs between the elastic strain energy, dissipative strain energy, and input strain energy. That is, with an increase in input strain energy, both the elastic strain energy and the dissipative strain energy increase linearly. The related fitting functions are shown in Table 3. Furthermore, the elastic strain energy grows faster than the dissipative strain energy. The difference between the elastic strain energy and dissipated energy gradually increases with increasing input strain energy. This shows that during the pre-peak rock loading process, with a certain amount of energy input from the outside world, most part is converted into the elastic strain energy, and a small part is consumed.

The R^2 of the fitting function is between 0.98 and 0.99, indicating that the fitting performance is good, and the linear relationships between elastic strain energy and dissipative strain energy and input strain energy are more reliable. In addition, rocks under various confining pressures conform to this linear energy relationships, which can be summarized into two general formulas:

$$U_k^e = a \times U_k^o + b \tag{6}$$

$$U_k^d = c \times U_k^o - b \tag{7}$$

where a, b and c are constants and c equals to (1-a). These two linear relationships are named as linear energy storage and dissipation laws. Moreover, b is very small relative to a and c, and the difference is two orders of magnitude, so b can be omitted in the formula. The general formula can be obtained after simplification:

$$U_k^e = a \times U_k^o \tag{8}$$

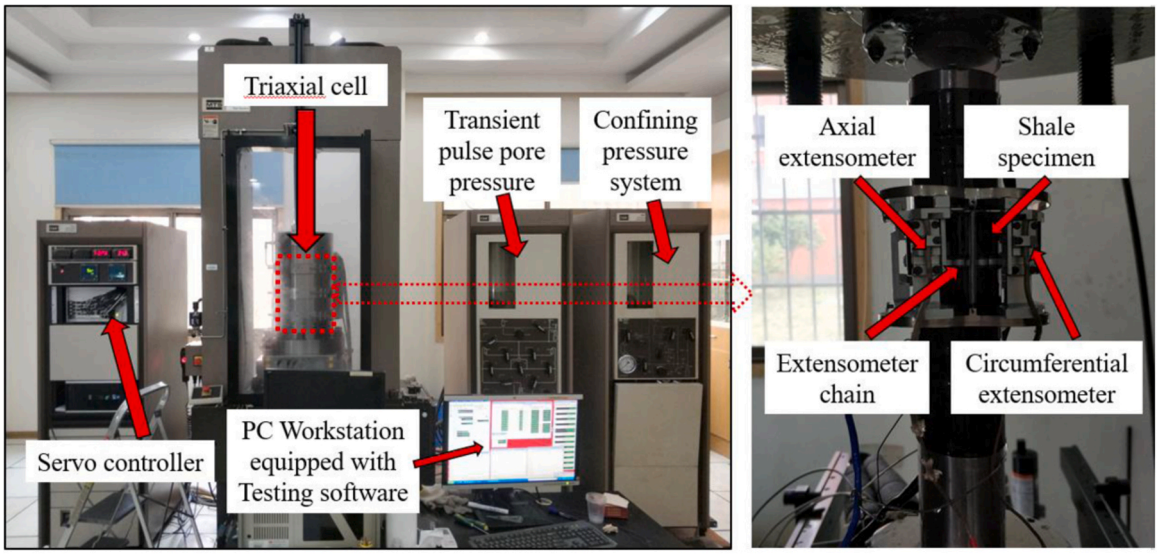

Fig. 4. MTS 815 rock mechanics test system.

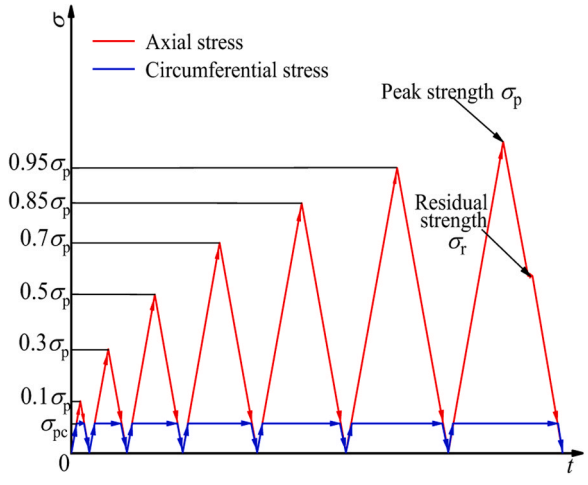

Fig. 5. Loading path of triaxial cyclic loading and unloading compression test.

$$U_k^d = c \times U_k^o \tag{9}$$

where a and c are the axial compression energy storage coefficient and the axial energy dissipation coefficient in the triaxial compression test, respectively.

4.2. Reliability verification of linear energy storage and dissipation laws

To verify the universality and reliability of the linear energy storage law, the data in other literatures are referred to for analysis and calculation [18,33]. In the literature, triaxial compression tests were carried out on red sandstone and granite. The strain energy parameters at each axial stress level were calculated through the experimental curves in the literature, and the energy evolution law in the process of rock deformation and failure was studied. The stress-strain curves of the red sandstone are shown in Fig. 8, and the elastic strain energy and dissipative strain energy curves of the granite are shown in Fig. 10. According to the experimental data, the relationships between the elastic strain energy, dissipative strain energy, and the input energy during the pre-peak loading were analyzed, as shown in Figs. 9 and 11. It can be observed that under different confining pressures, the elastic strain energy and dissipative strain energy of the two kinds of rocks have good linear relationships with the input strain energy. Through data fitting, it was found that the linear relationship did exist, and its coefficient of determination was between 0.94 and 0.99, indicating the reliability of the data fitting. The fitting equation, the coefficient of determination, and the ratio of intercept to slope are listed in Table 4. These results match the linear energy storage law obtained from the triaxial cyclic loading and unloading tests on shale in this work. The above analysis shows that the red sandstone and granite also conform to the linear energy storage and dissipation laws. In addition, previous studies have confirmed that there are similar energy storage and dissipation laws for different types of rocks under uniaxial compression, Brazilian splitting, shearing, and fracture conditions [19–21,4–6]. Therefore, the linear energy storage and dissipation laws are universal and can be regarded as one of the basic properties of rocks.

4.3. Calculation method of peak elastic strain energy and residual kinetic energy

According to the linear energy storage and dissipation laws obtained above, given the input energy of a certain stress level, the corresponding elastic strain energy and dissipative strain energy can be calculated more accurately. Based on this law, the peak elastic strain energy can be calculated accurately. This helps modify the rock brittleness index, thereby improving the judgment accuracy of the brittleness index.

Therefore, the calculation methods of the peak elastic strain energy and dissipative strain energy can be improved based on the linear energy storage law, so that BI_{ER} has better scientificity and accuracy. The peak elastic strain energy formula can be obtained as

$$U_p^e = a \times U_p^o + b \tag{10}$$

where U_p^e is the peak elastic strain energy; U_p^o is the peak input strain

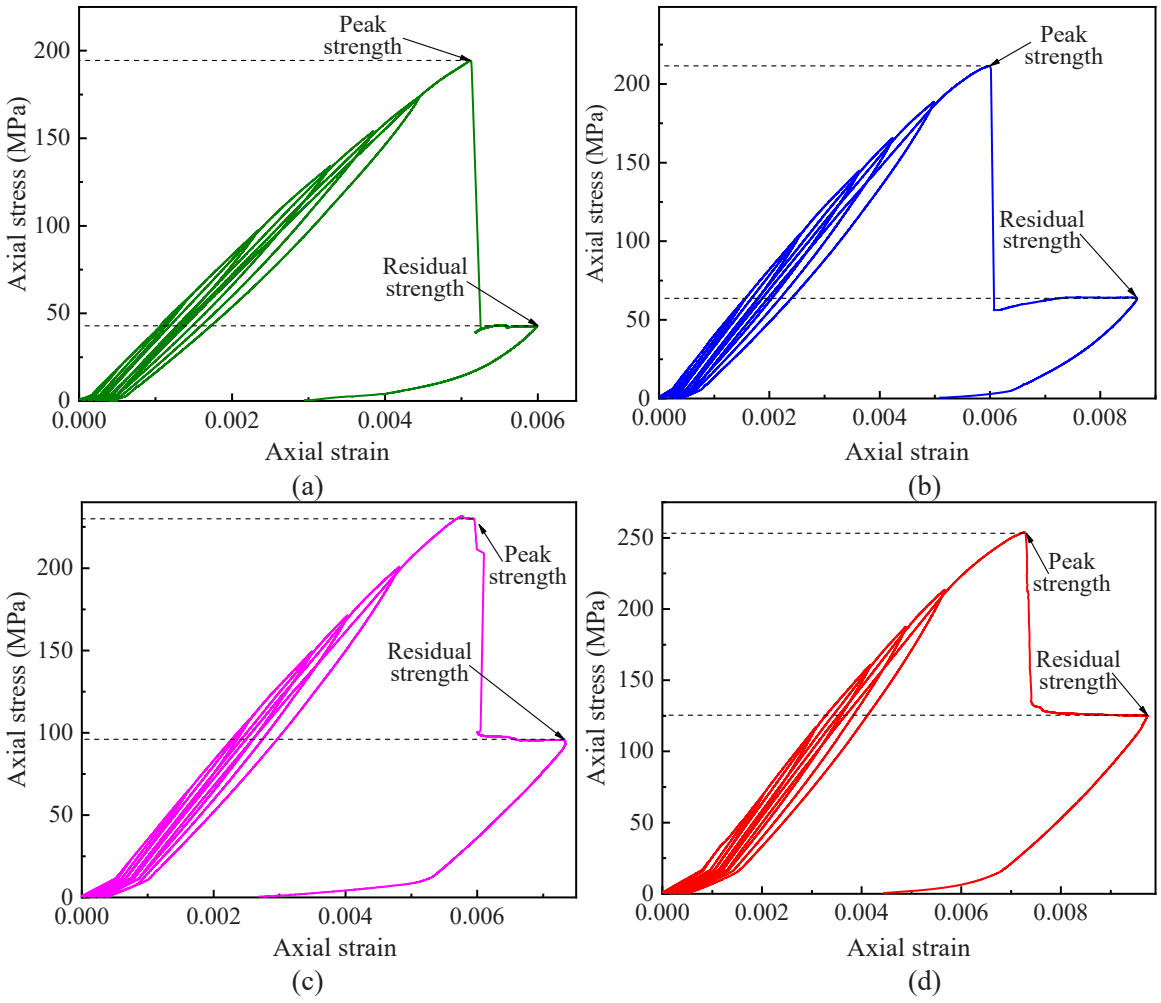

Fig. 6. Stress-strain curves of shale under different confining pressures: **(a)** 5 MPa, **(b)** 10 MPa, **(c)** 20 MPa, and **(d)** 30 MPa.

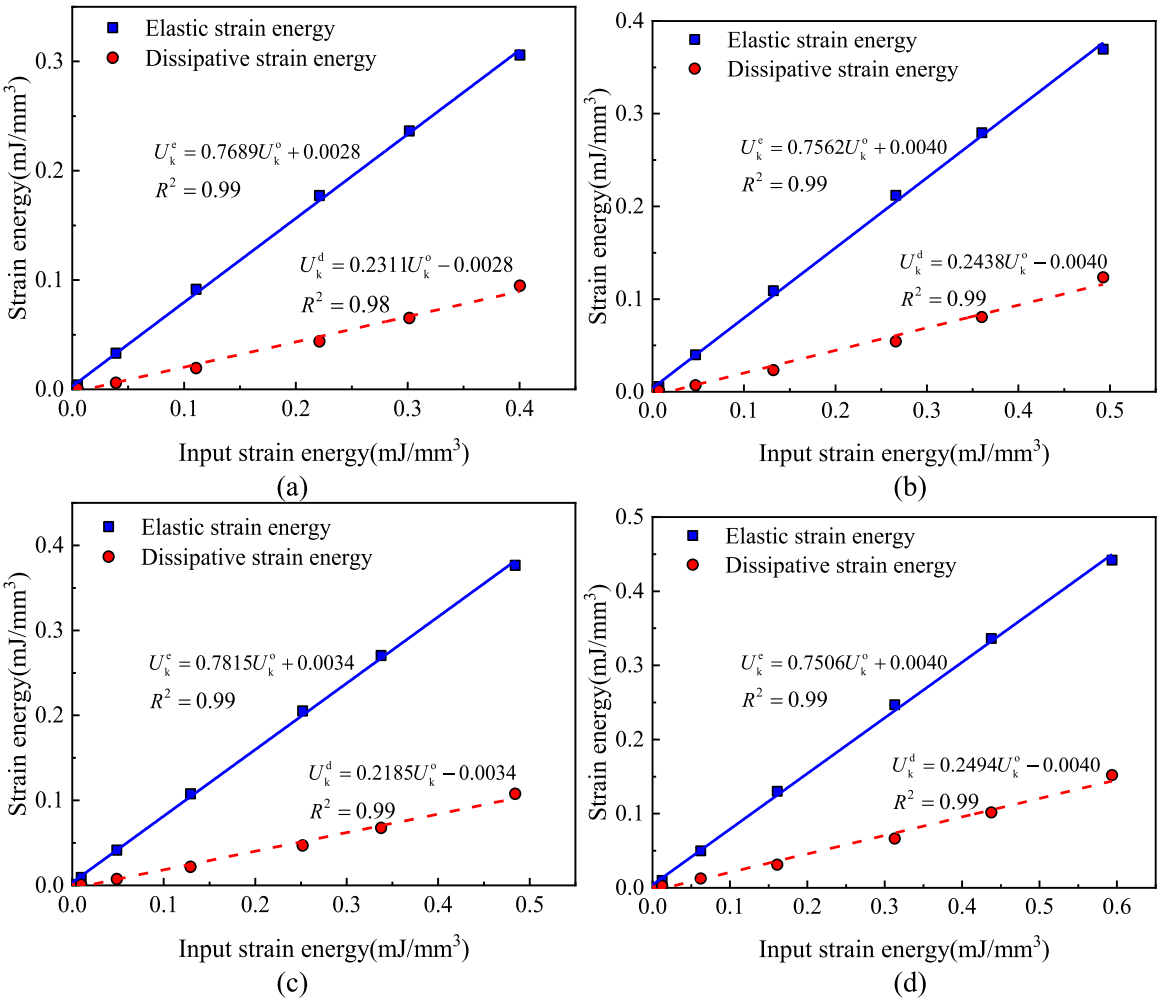

Fig. 7. The relationship between elastic strain energy and dissipative strain energy and input strain energy: **(a)** 5 MPa, **(b)** 10 MPa, **(c)** 20 MPa, and **(d)** 30 MPa.

Table 3
Fitted functional relationship between elastic strain energy and dissipative strain energy and input strain energy.

Confining Pressure/ MPa	Relationship between U_k^e,U_k^d andU_k^o	R^2	$\lvert b\rvert/a(\%)$or$\lvert b\rvert/c(\%)$
5	$U_k^e = 0.7689U_k^o + 0.0028$	0.99	0.40
	$U_k^d = 0.2311U_k^o - 0.0028$	0.98	1.21
10	$U_k^e = 0.7562U_k^o + 0.0040$	0.99	0.53
	$U_k^d = 0.2438U_k^o - 0.0040$	0.99	1.64
20	$U_k^e = 0.7815U_k^o + 0.0034$	0.99	0.44
	$U_k^d = 0.2185U_k^o - 0.0034$	0.99	1.56
30	$U_k^e = 0.7506U_k^o + 0.0040$	0.99	0.53
	$U_k^d = 0.2494U_k^o - 0.0040$	0.99	1.60

energy; U_p^o can be obtained by integrating the stress-strain curve, as follows:

$$U_p^o = \int_0^{\varepsilon_p} \sigma d\varepsilon \tag{11}$$

where ε_p is the axial strain at the rock peak strength. The corresponding peak dissipative strain energy U_p^d is the difference between the peak input energy and the peak elastic strain energy:

$$U_p^d = U_p^o - U_p^e \tag{12}$$

According to the above formulae, the improved peak elastic strain energy and peak dissipative strain energy can be obtained. To obtain the residual kinetic energy, it is necessary to conduct an in-depth analysis on the energy evolution characteristics of the rock in the residual strength stage. When the axial stress of the rock is maintained at the residual strength, the stress is unloaded at any point in this stage, and the area

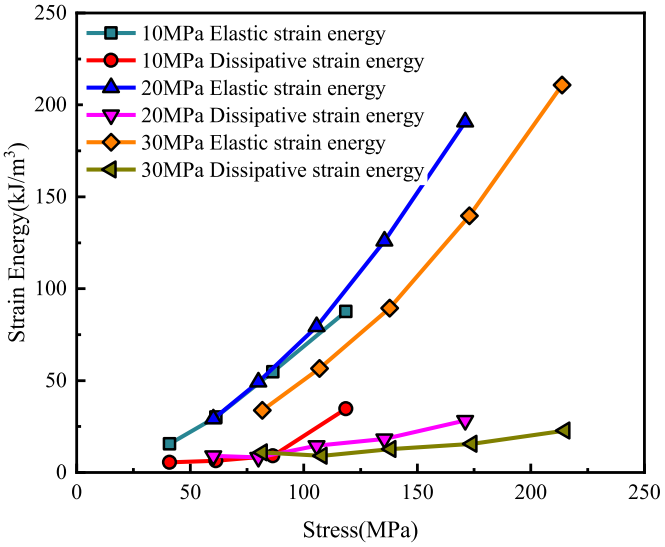

Fig. 10. Evolution curve of elastic strain energy and dissipative strain energy of granite [18].

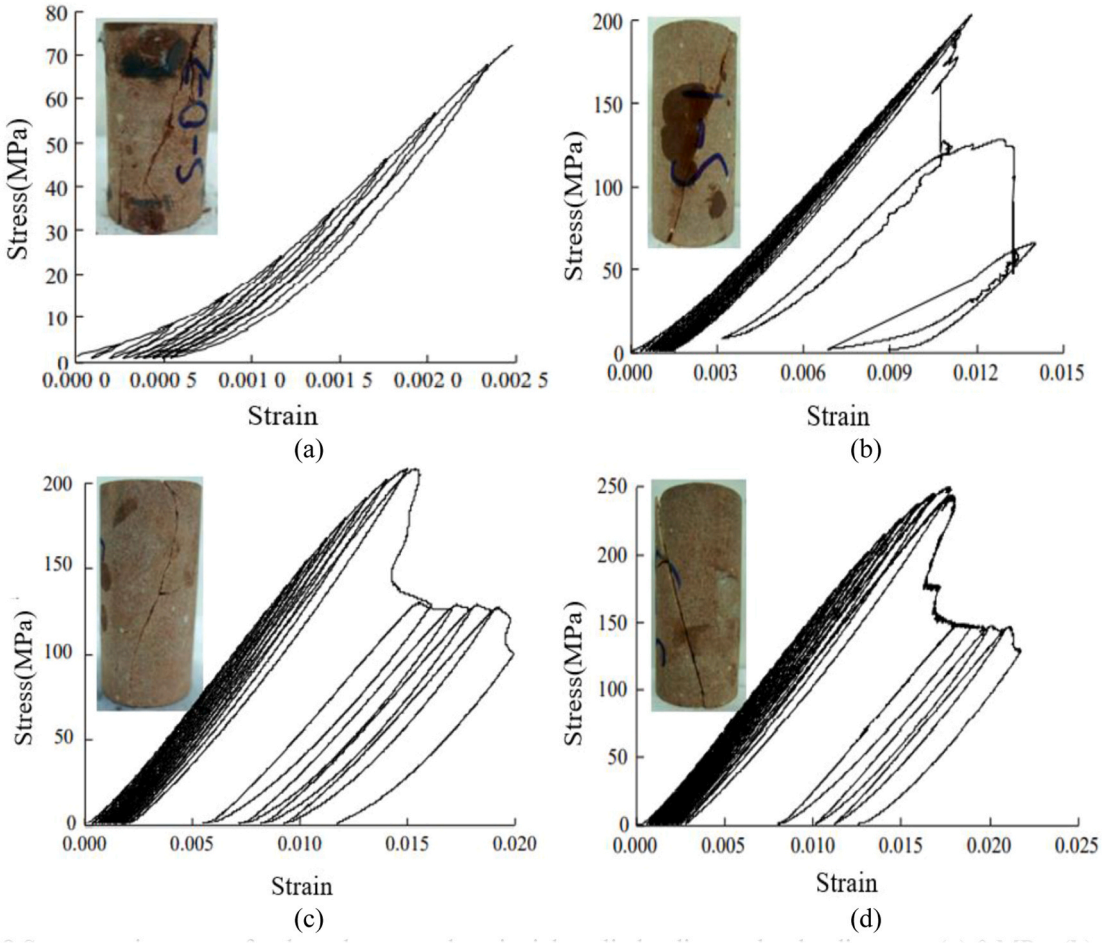

Fig. 8. Stress-strain curve of red sandstone under triaxial cyclic loading and unloading test: **(a)** 0 MPa, **(b)** 10 MPa, **(c)** 20 MPa, and **(d)** 30 MPa [33].

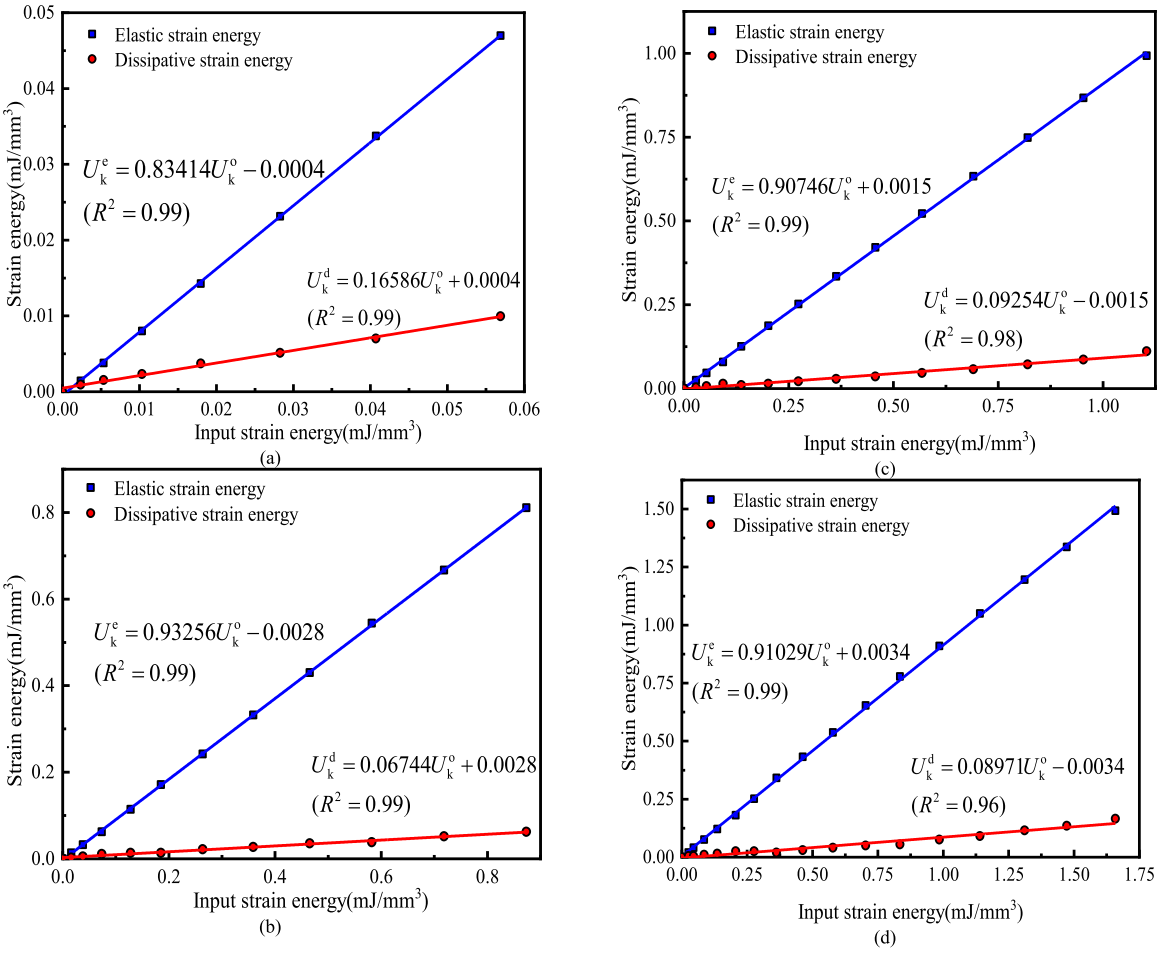

Fig. 9. The relationship between elastic strain energy, dissipative strain energy and input strain energy of red sandstone: **(a)** 0 MPa, **(b)** 10 MPa, **(c)** 20 MPa, and **(d)** 30 MPa.

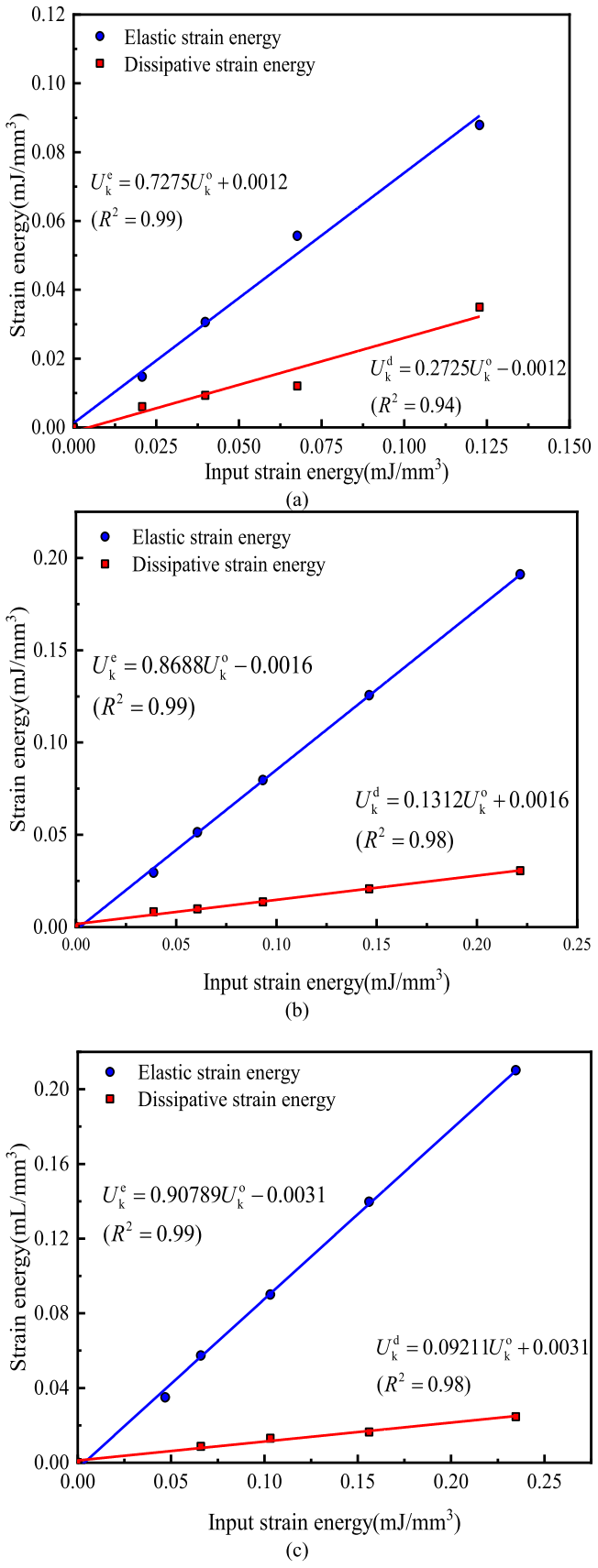

Fig. 11. The relationship between elastic strain energy, dissipative strain energy and input strain energy of granite: **(a)** 10 MPa, **(b)** 20 MPa, and **(c)** 30 MPa.

under the unloading curve represents the residual kinetic energy.

5. Improved peak elastic energy consumption ratio based on linear energy storage law

In this chapter, PEECR is improved according to the discovered linear energy storage law. And the accuracy and superiority of the improved PEECR are verified.

5.1. The improved peak elastic energy consumption ratio

Based on the linear energy storage law, BI_{ER} is improved. The improved brittleness index is expressed by $BI_{I\text{-}ER}$, which is consistent with BI_{ER} in the calculation formula. However, the peak elastic strain energy is calculated by the linear energy storage law.

When $\varepsilon_u > \varepsilon_p$, the improved brittleness index is determined as

$$BI_{I-ER} = \frac{a \times \int_0^{\varepsilon_p} \sigma d\varepsilon + b - \int_{\varepsilon_r}^{\varepsilon_p} \sigma d\varepsilon}{a \times \int_0^{\varepsilon_p} \sigma d\varepsilon + b} \tag{13}$$

When $\varepsilon_u < \varepsilon_p$, it is expressed by

$$BI_{I-ER} = \frac{a \times \int_0^{\varepsilon_p} \sigma d\varepsilon + b - \int_{\varepsilon_r}^{\varepsilon_p} \sigma d\varepsilon - 1\Big/2(\varepsilon_p - \varepsilon_u)^2 \times E}{a \times \int_0^{\varepsilon_p} \sigma d\varepsilon + b} \tag{14}$$

where E is the elastic modulus of the rock, $\varepsilon_p$is the axial strain at the peak strength, $\varepsilon_r$is the axial strain at the beginning of the residual strength stage, $\varepsilon_u$is axial strain at which the residual unloading stress is 0.

5.2. The accuracy and superiority of $BI_{I\text{-}ER}$

In order to verify whether the improved $BI_{I\text{-}ER}$ can judge the brittleness of rock accurately, the following data are calculated for the granite, shale and red sandstone in the triaxial cyclic loading and unloading compression test [31]. The stress-strain curves shown in Fig. 6, Fig. 8 and Fig. 12, and the calculations are listed in Table 5. The results show that the improved brittleness index $BI_{I\text{-}ER}$ gradually decreases as the confining pressure increases (Fig. 13). This is in line with the general law and shows that $BI_{I\text{-}ER}$ can accurately judge the brittleness of rocks.

To further verify the superiority of $BI_{I\text{-}ER}$, 11 existing energy-based rock brittleness indexes in Table 1 were compared. The $BI_{I\text{-}ER}$ and 11 brittleness indexes are used to judge the brittleness of tested shale to evaluate the judgment accuracy. The results of $BI_{I\text{-}ER}$ and other brittleness indexes under different confining pressures are shown in Fig. 14. In fact, the brittleness index except $BI_{I\text{-}ER}$ in Fig. 14 is more accurate in judging rock brittleness in specific fields, but there is no uniform standard to measure its accuracy. Therefore, the standard that rock brittleness decreases with increasing confining pressure can be used to judge the accuracy of brittleness index. It can be observed that the brittleness index except $BI_{I\text{-}ER}$ fluctuates with an increase in confining pressure, with no monotonic increase or decrease trend. In contrast, BI_{M-ER} always shows a decreasing trend with increasing confining pressure. Therefore, $BI_{I\text{-}ER}$ has better superiority and accuracy.

6. Conclusions

To obtain the peak elastic strain energy more accurately, the linear energy storage law of rock under triaxial cyclic loading and unloading compression test was analyzed. The BI_{ER} was improved according to the linear energy storage law, and the reliability of the improved index $BI_{I\text{-}ER}$ was verified by a series of data. The main conclusions are as follows:

1. The triaxial cyclic loading and unloading compression test was conducted on shale. It was found that the linear energy storage law existed in the shale, that is, the elastic strain energy increased

Table 4
Fitting function between elastic strain energy and dissipative strain energy of granite and red sandstone under different confining pressures.

Rock variety	Confining Pressure/MPa	Relationship between U_k^e, U_k^d and U_k^o	R^2	$\lvert b\rvert/a(\%)$ or $\lvert b\rvert/c(\%)$
Red sandstone	0	$U_k^e = 0.83414U_k^o - 0.0004$	0.99	0.04
		$U_k^d = 0.16586U_k^o + 0.0004$	0.99	0.24
	10	$U_k^e = 0.93256U_k^o - 0.0028$	0.99	0.30
		$U_k^d = 0.06744U_k^o + 0.0028$	0.99	4.15
	20	$U_k^e = 0.90746U_k^o + 0.0015$	0.99	0.17
		$U_k^d = 0.09254U_k^o - 0.0015$	0.98	1.62
	30	$U_k^e = 0.91029U_k^o + 0.0034$	0.99	0.37
		$U_k^d = 0.08971U_k^o - 0.0034$	0.96	3.89
Granite	10	$U_k^e = 0.7275U_k^o + 0.0012$	0.99	0.16
		$U_k^d = 0.2725U_k^o - 0.0012$	0.94	0.44
	20	$U_k^e = 0.8688U_k^o - 0.0016$	0.99	0.18
		$U_k^d = 0.1312U_k^o + 0.0016$	0.98	1.22
	30	$U_k^e = 0.90789U_k^o - 0.0031$	0.99	0.34
		$U_k^d = 0.09211U_k^o + 0.0031$	0.98	3.36

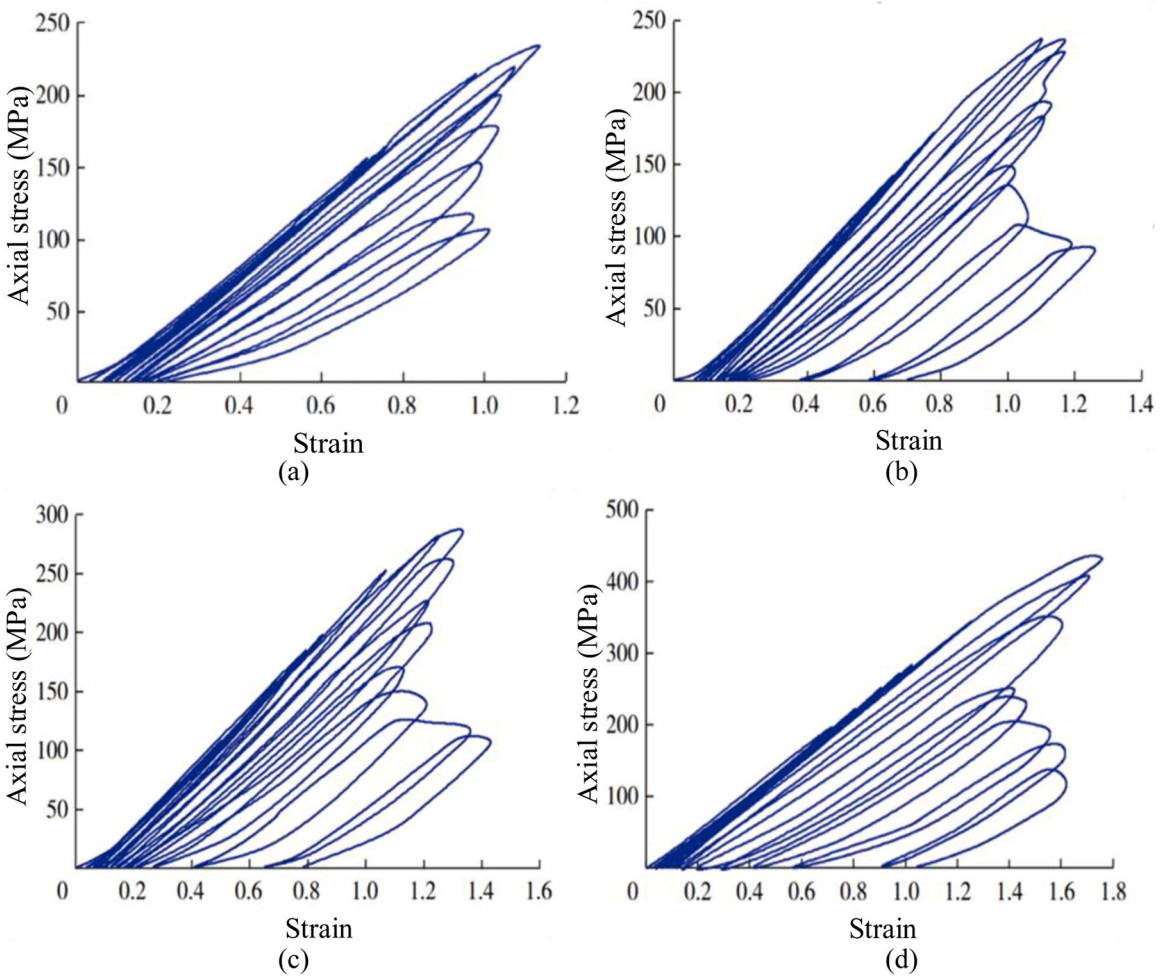

Fig. 12. Granite stress-strain curves under triaxial cyclic loading and unloading: **(a)** 5 MPa, **(b)** 10 MPa, **(c)** 15 MPa, and **(d)** 30 MPa [31].

Table 5
Values of BI_{I-ER} and BI_{ER} under different confining pressures of three rocks.

Rock type	Confining Pressure(MPa)	BI_{I-ER}	BI_{ER}
Granite	5	0.60	0.63
	10	0.48	0.52
	15	0.39	0.44
	30	0.25	0.29
Shale	5	0.88	0.94
	10	0.86	0.91
	20	0.69	0.78
	30	0.64	0.52
Red sandstone	0	0.79	0.84
	10	0.69	0.74
	20	0.44	0.54
	30	0.31	0.35

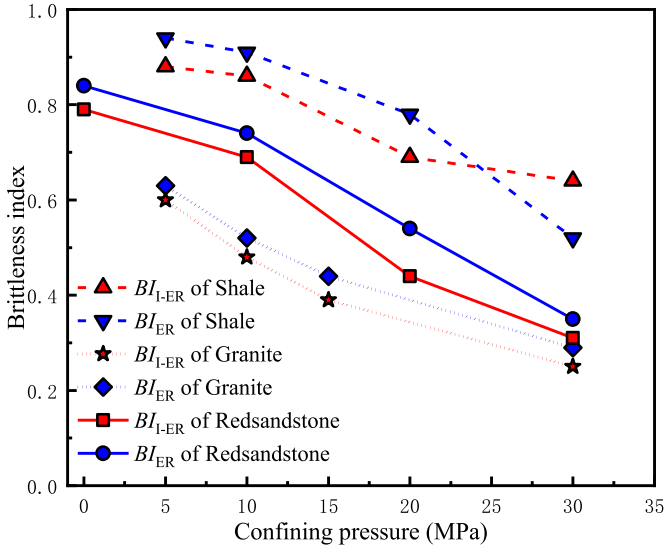

Fig. 13. Comparison of BI_{I-ER} and BI_{ER} of three rocks under different confining pressures.

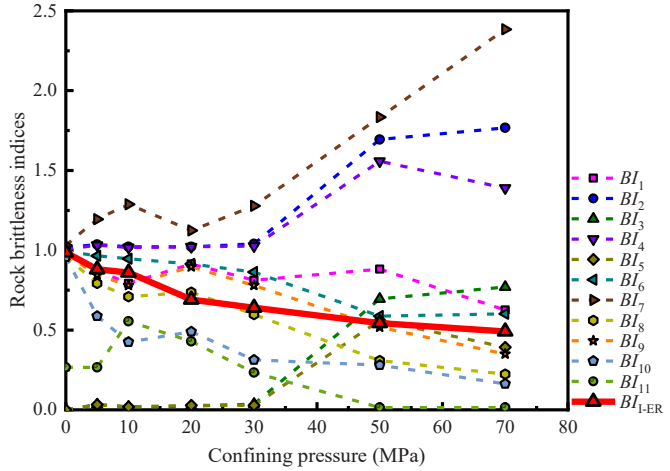

Fig. 14. Evaluation results of 11 existing brittleness indexes and BI_{I-ER} for shale specimens under different confining pressures.

linearly with increasing input strain energy. The universality of the linear energy storage law was verified using the triaxial cyclic loading and unloading compression test curves in the published literature.

2. The BI_{ER} is improved based on the linear energy storage law and named as BI_{I-ER}. The BI_{I-ER} is calculated by a series of stress-strain curves in the triaxial cyclic loading and unloading compression test. Compared with the 11 existing brittleness indexes, the BI_{I-ER} can evaluate rock brittleness more accurately.

Declaration of Competing Interest

We declare that we do not have any commercial or associative interest that represents a conflict of interest in connection with the work submitted. The manuscript is approved by all authors for publication.

Acknowledgments

This work was supported by the National Natural Science Foundation of China (Grant No. 42077244).

References

[1] R. Altindag, The evaluation of rock brittleness concept on rotary blast hole drills, J. S Afr. Inst. Min. Metallurgy 102 (1) (2002) 61–66.
[2] C. Ai, J. Zhang, Y.W. Li, J. Zeng, X.L. Yang, J.G. Wang, Estimation criteria for rock brittleness based on energy analysis during the rupturing process, Rock Mech. Rock Eng. 49 (2016) 4681–4698.
[3] X. Gong, C.C. Sun, A new tablet brittleness index, Eur.J. Pharm. Biopharm. 93 (2015) 260–266.
[4] F.Q. Gong, J.Y. Yan, X.B. Li, A new criterion of rock burst proneness based on the linear energy storage law and the residual elastic energy index, Chin. J Rock Mech. Eng. 37 (9) (2018) 1993–2014.
[5] F.Q. Gong, S. Luo, J.Y. Yan, Energy storage and dissipation evolution process and characteristics of marble in three tension-type failure tests, Rock Mech. Rock Eng. 51 (2018) 3613–3624.
[6] F.Q. Gong, J.Y. Yan, S. Luo, X.B. Li, Investigation on the linear energy storage and dissipation laws of rock materials under uniaxial compression, Rock Mech. Rock Eng. 52 (2019) 4237–4255.
[7] F.Q. Gong, Y.L. Wang, A new rock brittleness index based on the peak elastic strain energy consumption ratio, Rock Mech. Rock Eng. 55 (3) (2022) 1583–1584.
[8] S.F. Guo, S.W. Qi, Z.F. Zhan, B.W. Zheng, Plastic-strain-dependent strength model to simulate the cracking process of brittle rocks with an existing non-persistent joint, Eng. Geol 231 (2017) 114–125.
[9] V. Hucka, B. Das, Brittleness determination of rocks by different methods, Int. J. Rock Mech. Min. Sci. Geomech. Abstr. 11 (10) (1974) 389–392.
[10] Z.P. Huo, J.C. Zhang, P. Li, X. Tang, X. Yang, Q.L. Qiu, Z. Dong, Z. Li, An improved evaluation method for the brittleness index of shale and its application—a case study from the southern north China basin, J. Nat. Gas Sci. Eng. 59 (2018) 47–55.
[11] M. Khandelwal, R.S. Faradonbeh, M. Monjezi, D.J. Armaghani, M.Z. Majid, Function development for appraising brittleness of intact rocks using genetic programming and non-linear multiple regression models, Eng. Comput. 33 (1) (2017) 13–21.
[12] I.R. Kivi, M. Ameri, H. Molladavoodi, Shale brittleness evaluation based on energy balance analysis of stress-strain curves, J. Pet Sci. Eng. 167 (2018) 1–19.
[13] Z.H. Kuang, S.L. Qiu, S.J. Li, S.H. Du, Y. Huang, X.Q. Chen, A new rock brittleness index based on the characteristics of complete stress-strain behaviors, Rock Mech. Rock Eng. 54 (10) (2021) 1109–1128.
[14] Q.H. Li, M. Chen, Y. Jin, B. Hou, B.W. Zhang, Laboratory evaluation method and improvement of shale brittleness, Chin. J. Rock Mech. Eng. 31 (08) (2012) 1680–1685.
[15] N. Li, Y.S. Zou, S.C. Zhang, X.F. Ma, X.W. Zhu, S.H. Li, T. Cao, Rock brittleness evaluation based on energy dissipation under triaxial compression, J. Pet Sci. Eng. 183 (2019) 1–10.
[16] L.C. Li, M.Y. Zhai, L.Y. Zhang, Z.L. Zhang, B. Huang, A.L. Li, J.Q. Zuo, Q.S. Zhang, Brittleness evaluation of glutenite based on energy balance and damage evolution, Energies 12 (18) (2019) 1–28.
[17] Y.W. Li, L.H. Zhou, D.P. Li, S.C. Zhang, F.C. Tian, Z.M. Xie, B. Liu, Shale brittleness index based on the energy evolution theory and evaluation with logging data: a case study of the Guandong block, ACS Omega 5 (2020) 13164–13175.
[18] Y.Y. Liu, S.J. Miao, X. Wei, G.J. Cui, H. Wang, Acoustic emission characteristics and energy mechanism evolution of granite damage under triaxial cyclic loading and unloading, Min. Res. Dev 36 (06) (2016) 68–72.
[19] S. Luo, F.Q. Gong, Linear energy storage and dissipation laws during rock fracture under three-point flexural loading, Eng. Fract. Mech. 234 (2020) 107102.
[20] S. Luo, F.Q. Gong, Linear energy storage and dissipation laws of rocks under preset angle shear conditions, Rock Mech. Rock Eng. 53 (10) (2020) 3303–3323.

[21] S. Luo, F.Q. Gong, Evaluation of energy storage and release potentials of highly stressed rock pillar from rockburst control perspectives, Int. J. Rock Mech. Min. Sci. 163 (2023) 105324.
[22] F.Z. Meng, L.N.Y. Wong, H. Zhou, Rock brittleness indices and their applications to different fields of rock engineering: a review, J. Rock Mech. Geotech. 13 (2020) 221–247.
[23] Q.B. Meng, C.K. Wang, B.X. Huang, H. Pu, Z.Z. Zhang, W. Sun, J. Wang, Rock energy evolution and distribution law under triaxial cyclic loading and unloading conditions, Chin. J. Rock Mech. Eng. 39 (10) (2020) 2047–2059.
[24] H.Q. Song, J.P. Zuo, Y. Chen, L.Y. Li, Z.J. Hong, Revised energy drop coefcient based on energy characteristics in whole process of rock failure, Rock Soil Mech. 40 (1) (2019) 91–98.
[25] B.G. Tarasovn, M.F. Randolph, Superbrittleness of rocks and earthquake activity, Int. J. Rock Mech. Min. Sci. 48 (2011) 888–898.
[26] B.G. Tarasovn, Y. Potvin, Universal criteria for rock brittleness estimation under triaxial compression, Int. J. Rock Mech. Min. Sci. 59 (2013) 57–69.
[27] Y. Wang, X. Li, Y.F. Wu, Y.X. Ben, D.S. Li, J.M. Hao, B. Zhang, Discussion on the relationship between crack initiation stress level and brittleness index of brittle rock, Chin. J. Rock Mech. Eng. 33 (02) (2014) 264–275.
[28] Xia Y.J. (2017) Improvement of rock brittleness evaluation method and its numerical test research, Dalian University of Technology.
[29] Y.J. Xia, L.C. Li, C.A. Tang, X.Y. Li, S. Ma, M. Li, A new method to evaluate rock mass brittleness based on stress–strain curves of class I, Rock Mech. Rock Eng. 50 (2017) 1123–1139.
[30] H.P. Xie, Y. Ju, L.Y. Li, R.D. Peng, Energy mechanism of deformation and failure of rock mass, Chin. J. Rock Mech. Eng. 27 (9) (2008) 1729–1740.
[31] J.X. Yang, M.K. Luo, X.W. Zhang, N. Huang, S.J. Hou, Study on mechanical properties and fatigue damage evolution of granite under cyclic loading and unloading conditions, J. Min. Strata Control Eng. 3 (03) (2021) 91–98.
[32] H. Zhou, F.Z. Meng, C.Q. Zhang, R.C. Xu, J.J. Lu, Quantitative evaluation method of rock brittleness characteristics based on stress-strain curve, Chin. J. Rock Mech. Eng. 33 (06) (2014) 1114–1122.
[33] Z.Z. Zhang, F. Gao, Research on confining pressure effects on energy evolution of loaded rocks, Chin. J. Rock Mech. Eng. 34 (01) (2015) 1–11.

Fengqiang Gong, professor and doctoral supervisor of Southeast University, provincial high-level leading talent, concurrently serves as a member of the Commission on Rockburst of the International Society of Rock Mechanics and Rock Engineering, the vice chairman of the Commission on Rock Crushing Engineering of the Chinese Society of Rock Mechanics and Engineering, the vice chairman of the Deep Earth Mining Construction and Resource Development Special Committee of the Chinese Society of Nonferrous Metals, and the member of the Commission on the Prevention and Control of Coalburst and Rockburst of the China Mine Safety Society. He has published more than 60 SCI papers as the first/corresponding author, including 15 ESI highly cited papers, 8 hot papers, and an H-index of 44. He has been selected into the list of the world's top 2% scientists and Elsevier China Highly Cited Scholar. He is a member of the editorial board of Acta Geophysica, Journal of Central South University, Chinese Journal of Rock Mechanics and Engineering, Journal of Mining and Rock Formation Control Engineering, Journal of Engineering Geology, Nonferrous Metals (Mining Part).

Yiru Zuo, graduated from Huazhong University of Science and Technology with a bachelor's degree, and entered Southeast University in September 2021 to study for a master's degree, and the supervisor is Professor Fengqiang Gong. The main research direction is the experimental study of the energy storage and consumption law and rockburst tendency of bedding shale.